Defence Science Journal, Vol. 63, No. 5, September 2013, pp. 508-514, DOI : 10.14429/dsj.63.2458

Application of Metallic Strip Gratings for Enhancement of Electromagnetic Performance of A-sandwich Radome

Raveendranath U. Nair*, J. Madhumitha, and R.M. Jha
CSIR-National Aerospace Laboratories, Bangalore - 560 017, India
**E-mail: raviunair@nal.res.in*

ABSTRACT

Enhancement of the electromagnetic (EM) performance characteristics of A-sandwich radome wall over X-band using metallic strip gratings is presented in this work. Equivalent transmission line method in conjunction with equivalent circuit model (ECM) is used for modeling the A-sandwich radome panel with metallic strip gratings and the computation of radome performance parameters. Metallic strip grating embedded in the mid-plane of the core and those in the skin-core interface are the configurations considered in the present work. For a given thickness of metallic strip grating, its width and pitch are optimized at different angles of incidence such that the new radome wall configuration offers superior EM performance over the entire X-band as compared to the conventional A-sandwich wall. The EM analysis shows that the superior EM performance of A-sandwich with metallic strip gratings makes it suitable for the design of normal incidence and streamlined airborne radomes.

Keywords: Radomes, metallic strip gratings, radome performance parameters

NOMENCLATURE

β	Constant
ε_r	Dielectric constant
Φ	Electrical length
λ	Wavelength
θ	Incidence angle
A, B, C, D	Elements of transmission matrix
B_G	Shunt susceptance of the metallic strip gratings
C_n	Coefficients of n^{th} order
P_{tr}	Power transmission coefficient
P_{rf}	Power reflection coefficient
P	Pitch
tan δ_e	Electric loss tangent
t_{ms}	Thickness of metallic strip
t_{c1}	Thickness of core for configuration *1*
t_{c2}	Thickness of core for configuration *2*
t_p	Thickness of radome paint layer
t_s	Thickness of skin layer
T_1, T_2	Voltage transmission coefficients
w	Width of the strip
Z_0	Impedance of free space
Z_c	Impedance of core layer
Z_p	Impedance of paint layer
Z_s	Impedance of skin layer

1. INTRODUCTION

The stringent electromagnetic (EM) performance requirements of modern airborne radar systems require novel radome designs. Many techniques based on metallic structures (wire grids, wire meshes, etc.), anisotropic inclusions, and resonant/ semi-resonant structures were reported for modifying the radome wall configurations to enhance the EM performance of radome walls[1-4]. Monolithic radome panels, centrally loaded by a periodic array of conducting inclusions, offered a wider frequency bandwidth compared to the conventional radome designs of the same material and thickness[5]. Frequency selective surfaces (FSS) find potential applications in the design of high performance radomes due to their inherent frequency selective characteristics[6-8]. Recently reported works show that metamaterial-based FSS structures are used in the design of novel radome wall configurations[9-11]. In airborne radome applications, A-sandwich radome wall configuration is generally preferred to monolithic wall due to high strength-to-weight ratio and bandwidth[12]. However the EM performance of conventional A-sandwich wall may not be sufficient to meet the requirements of modern radome applications. Hence in the present work, novel designs based on metallic strip gratings are used to enhance the EM performance of A-sandwich radome for airborne applications. Since metallic strips considered in the present work are thin (thickness = 0.1 mm), it is easy to load them in the layers of A-sandwich wall.

The A-sandwich radome wall considered here is composed of three layers namely, outer skin, core and inner skin. The outer and inner skin layers are made of glass-epoxy, while the core is made of polyurethane foam. The core thickness is optimized for maximum power transmission over the X-band. In order to enhance the EM performance, the metallic strip gratings consisting of planar array of strips are either fixed on the surfaces or embedded in the layers. The design configurations with metallic strip gratings studied are:

(i) metallic strip gratings embedded in the mid-plane of the core layer (Configuration 1) and

Received 20 June 2012, revised 22 August 2013, online published 25 September 2013

(ii) metallic strip gratings embedded in each skin-core interface (Configuration 2).

For each configuration mentioned above as shown in Fig. 1, the optimum design parameters of the metallic strip gratings and radome EM performance parameters are computed based on the equivalent transmission line method in conjunction with equivalent circuit model.

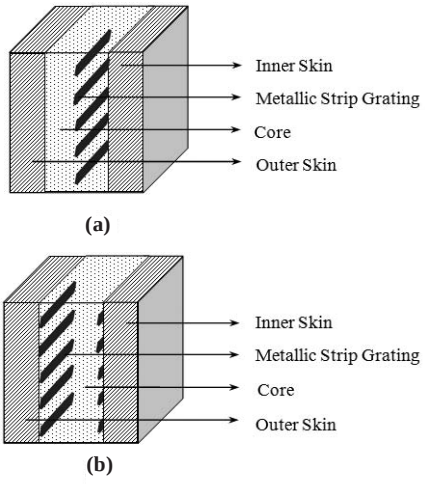

Figure 1. Schematic of A-sandwich radome panel with metallic strip gratings (a) embedded in the mid-plane of the core (Configuration 1) and (b) embedded in each skin-core interface (Configuration 2).

Further EM performance parameters (power transmission, power reflection and insertion phase delay) of both novel radome wall configurations with metallic strip gratings and A-sandwich alone structure are evaluated for perpendicular polarization over a range of incidence angles from normal incidence to high incidence angle 80°. The EM analysis shows that the A-sandwich radome wall with metallic strip gratings have superior EM performance as compared to conventional A-sandwich wall. The results indicate that these configurations have potential applications in the design of both normal incidence and highly streamlined airborne radomes.

2. EM DESIGN ASPECTS OF A-SANDWICH RADOME WALL CONFIGURATION WITH METALLIC STRIP GRATINGS

The A-sandwich radome wall is composed of three layers namely, outer skin, core and inner skin. The outer and inner skin layers considered are made of glass-epoxy (dielectric constant, $\varepsilon_r = 4$; and loss tangent, $\tan \delta_e = 0.015$) with constant thickness of 0.75 mm for structural rigidity. The core is made of polyurethane foam ($\varepsilon_r = 1.15$ and $\tan \delta_e = 0.005$) with optimized thickness of 5.84 mm for maximum power transmission over the X-band. The surface of the outer skin layer is coated with a radome paint ($\varepsilon_r = 3.46$ and $\tan \delta_e = 0.068$) of thickness 0.2 mm. The metallic strip grating consists of a planar array of thin parallel strips of uniform cross-section. The thickness of the metallic strip is assumed to be very small (of the order of 0.1 mm).

The wavelengths corresponding to low frequency edge (8 GHz) and high frequency edge (12 GHz) of X-band are 37.5 mm and 25 mm, respectively. It is obvious that the optimized core thickness considered in the present work is less than quarter wavelength corresponding to the above mentioned lower and upper frequency limits of X-band. The susceptance of a dielectric layer with thickness less than quarter wavelength is purely capacitive[4]. If the capacitive susceptance of the core can be cancelled out by proper inductive loading within the core using suitable metallic structures, superior EM performance characteristics over broadband of frequencies can be achieved. In this paper, the inductive loading within the core is achieved by embedding the array of metallic strips in the mid-plane of the core (Configuration 1) or at the core-skin interface (Configuration 2). The EM design strategy involved is that the design parameters (pitch and width, keeping constant thickness) of the metallic strip grating matches with the capacitive susceptance of the entire A-sandwich radome wall. Hence the resulting structure acts as spatial low-pass filter, providing superior EM performance over the entire X-band. The metallic strip gratings are very sensitive to the polarization and angle of incidence. For the configurations considered in the work, the design parameters of the metallic strip gratings (width and pitch) and radome EM performance parameters are computed based on the equivalent transmission line method[13,14] in conjunction with equivalent circuit model[15]. It is observed that for a given radome wall configuration with identical materials and dimensions, the radome EM performance characteristics are generally superior for parallel polarization, as compared to perpendicular polarization at a given incidence angle. This is due to the fact that the wave impedance for parallel polarization is less than that of perpendicular polarization at a given incidence angle. In other words, the performance degradations for a given radome wall configuration may be more for the perpendicular polarization case as compared to the parallel polarization case.

Hence in the present work, the EM performance parameters are analyzed and reported only for perpendicular polarization, which is capable of catering to the worst-case scenarios.

The metallic strip grating incorporated A-sandwich radome wall is considered as an equivalent transmission line with different sections corresponding to slab and metallic strip grating structure (Fig. 1). The change in the characteristic impedance of the free space and A-sandwich wall is a major source of reflection of the wave incident on the structure. As compared to the free space, different layers of radome wall can be considered as low impedance lines connected end to end. Hence the whole configuration can be represented by a single matrix obtained by the multiplication of matrices corresponding to the individual layers.

For Configuration 1 (Fig. 1(a)), the matrix representing each layer of A-sandwich wall are as follows.

The inner skin is represented by

$$\begin{bmatrix} A_1 & B_1 \\ C_1 & D_1 \end{bmatrix} = \begin{bmatrix} \cos\Phi_1 & j\dfrac{Z_s}{Z_o}\sin\Phi_1 \\ j\dfrac{Z_o}{Z_s}\sin\Phi_1 & \cos\Phi_1 \end{bmatrix} \quad (1)$$

In Configuration 1, the metallic strip grating is located at the mid-plane of the core. Hence the core can be considered

to be made up of two identical sections with strip grating in between them. Then the half-section of the core is represented by

$$\begin{bmatrix} A_2 & B_2 \\ C_2 & D_2 \end{bmatrix} = \begin{bmatrix} \cos\Phi_2 & j\frac{z_c}{z_o}\sin\Phi_2 \\ j\frac{z_o}{z_c}\sin\Phi_2 & \cos\Phi_2 \end{bmatrix} \quad (2)$$

Let $A_{MS,}$ B_{MS}, C_{MS} and D_{MS} be the elements of the matrix representing metallic strip grating

$$\begin{bmatrix} A_{MS} & B_{MS} \\ C_{MS} & D_{MS} \end{bmatrix} = \begin{bmatrix} 1 & 0 \\ jB_G & 1 \end{bmatrix} \quad (3)$$

Here B_G represents the shunt susceptance of the metallic strip grating[15]. For perpendicular polarization, the shunt susceptance of the strip for perpendicular polarization is given by

$$B_G = \frac{-4p\sec\theta}{\lambda}\left[(\ln\cos ec\,(\frac{\pi g}{2p}) + G\right] \quad (4)$$

Here the correction term is given by

$$G = \frac{0.5(1-\beta^2)^2\left[(1-\frac{\beta^2}{4})(C_{1+}+C_{1-}) + 4\beta^2 C_{1+}C_{1-}\right]}{(1-\frac{\beta^2}{4}) + \beta^2(1+\frac{\beta^2}{2}-\frac{\beta^4}{8})(C_{1+}+C_{1-}) + 2\beta^6 C_{1+}C_{1-}} \quad (5)$$

The coefficients are given by

$$C_{1\pm} = \frac{1}{\sqrt{(\frac{p\sin\theta}{\lambda}\pm 1)^2 - \frac{p^2}{\lambda^2}}} - 1 \quad (6)$$

Here $\beta = \sin\left(\frac{\pi w}{2p}\right)$ and n = ±1, ±2, ±3,……..

The other half-section of the core is represented by

$$\begin{bmatrix} A_3 & B_3 \\ C_3 & D_3 \end{bmatrix} = \begin{bmatrix} \cos\Phi_3 & j\frac{z_c}{z_o}\sin\Phi_3 \\ j\frac{z_o}{z_c}\sin\Phi_3 & \cos\Phi_3 \end{bmatrix} \quad (7)$$

The outer skin is represented by

$$\begin{bmatrix} A_4 & B_4 \\ C_4 & D_4 \end{bmatrix} = \begin{bmatrix} \cos\Phi_4 & j\frac{z_s}{z_o}\sin\Phi_4 \\ j\frac{z_o}{z_s}\sin\Phi_4 & \cos\Phi_4 \end{bmatrix} \quad (8)$$

The radome paint is represented by

$$\begin{bmatrix} A_5 & B_5 \\ C_5 & D_5 \end{bmatrix} = \begin{bmatrix} \cos\Phi_5 & j\frac{z_p}{z_o}\sin\Phi_5 \\ j\frac{z_o}{z_p}\sin\Phi_5 & \cos\Phi_5 \end{bmatrix} \quad (9)$$

Thus, the entire A-sandwich configuration with metallic strip grating embedded at the mid-plane of the core may be expressed as

$$\begin{bmatrix} A & B \\ C & D \end{bmatrix} = \begin{bmatrix} A_1 & B_1 \\ C_1 & D_1 \end{bmatrix}\begin{bmatrix} A_2 & B_2 \\ C_2 & D_2 \end{bmatrix}\begin{bmatrix} 1 & 0 \\ jB_G & 1 \end{bmatrix}\begin{bmatrix} A_3 & B_3 \\ C_3 & D_3 \end{bmatrix}\begin{bmatrix} A_4 & B_4 \\ C_4 & D_4 \end{bmatrix}\begin{bmatrix} A_5 & B_5 \\ C_5 & D_5 \end{bmatrix} \quad (10)$$

In Configuration 2, metallic strip grating is embedded in each skin-core interface (Fig. 1(b)). Then the entire A-sandwich radome wall with metallic strip gratings is represented by

$$\begin{bmatrix} A & B \\ C & D \end{bmatrix} = \begin{bmatrix} A_1 & B_1 \\ C_1 & D_1 \end{bmatrix}\begin{bmatrix} 1 & 0 \\ jB_G & 1 \end{bmatrix}\begin{bmatrix} A_2 & B_2 \\ C_2 & D_2 \end{bmatrix}\begin{bmatrix} 1 & 0 \\ jB_G & 1 \end{bmatrix}\begin{bmatrix} A_4 & B_4 \\ C_4 & D_4 \end{bmatrix}\begin{bmatrix} A_5 & B_5 \\ C_5 & D_5 \end{bmatrix} \quad (11)$$

Here $\begin{bmatrix} A_2 & B_2 \\ C_2 & D_2 \end{bmatrix}$ represents the core of the radome wall, which is different from that of Configuration 1.

Using Eqns (10) and (11), the *A, B, C,* and *D* parameters of the final matrix are computed for each Configuration. The power transmission coefficient is given by

$$P_{tr} = \left[\frac{4}{(A+B+C+D)^2}\right] \quad (12)$$

The power reflection coefficient is given by

$$P_{rf} = \left[\frac{A+B-C-D}{A+B+C+D}\right]^2 \quad (13)$$

The phase distortions are determined by the insertion phase delay (IPD) of the radome wall. For the Configuration *1*, two skin layers, cores sections, metallic strip grating and radome paint are cascaded. Hence the insertion phase delays for Configuration 1 is given by

$$IPD_1 = -\angle T_1 - \frac{2\pi}{\lambda}\left(2t_s + 2t_{c1} + t_{ms} + t_p\right)\cos\theta \quad (14)$$

Similarly, insertion phase delay for Configuration 2 is given by

$$IPD_2 = -\angle T_2 - \frac{2\pi}{\lambda}\left(2t_s + t_{c2} + 2t_{ms} + t_p\right)\cos\theta \quad (15)$$

Here $\angle T_1$ and $\angle T_2$ are the phase angles associated with the voltage transmission coefficients corresponding to Configuration 1 and Configuration 2 respectively. The thicknesses of skin layers, metallic strip grating and radome paint are given by t_s, $t_{ms,}$ and t_p respectively. Let t_{c1} be the thickness of each section of the core for Configuration 1, while t_{c2} be the core thickness for Configuration 2.

3. EM PERFORMANCE ANALYSIS OF A-SANDWICH STRUCTURE WITH METALLIC STRIP GRATINGS

A comparative study of the EM performance of A-sandwich wall with metallic strip gratings and A-sandwich wall alone is carried out for Configuration 1. The EM performance parameters are computed at normal incidence, 45°, 60°, and 80° for perpendicular polarization over X-band frequency range. The optimized design parameters of metallic strip gratings for Configuration 1 are given in Table 1. Figures 2-4 show the EM performance characteristics of Configuration 1. It may be observed that the A-sandwich wall with metallic strip grating shows superior power transmission characteristics as compared to A-sandwich wall alone (Fig. 2). The power transmission of the A-sandwich wall embedded with strip grating is well above 90 per cent at normal incidence, 45°, and 60°. But there is degradation of power transmission efficiency at high incidence angle 80°. The power reflection is very low (a desirable characteristic) for the A-sandwich wall with

strip grating as compared to the A-sandwich alone wall (Figs. 3(a) and 3(d)). It is observed that the power reflection of the conventional A-sandwich structure increases with the increase in the incidence angle. TThe insertion phase delay (IPD) characteristics are shown in Figs. 4(a) and 4(d). It is observed that the IPD of the A-sandwich wall embedded with strip gratings is same as that of the conventional structure at normal incidence. However, the IPD of the strip embedded structure increases with incidence angle.

The EM performance parameters of A-sandwich wall with metallic strip gratings embedded in each skin-core interface (Configuration 2) and A-sandwich wall alone are shown in Figs. 5 and 7. The optimized design parameters of metallic strip gratings corresponding to Configuration 2 are given in Table 1. Figure 5 show the power transmission characteristics of Configuration 2 at normal incidence, 45°, 60°, and 80°. It is noted that the inclusion of metallic strip gratings at each skin-core interface improves the power transmission efficiency. The A-sandwich wall with strip gratings shows excellent power transmission characteristics (above 90%) at normal incidence. There is degradation in the power transmission efficiency of the A-sandwich wall with strip gratings at other incidence angle. However, the power transmission characteristics of A-sandwich wall with strip gratings are better than that of

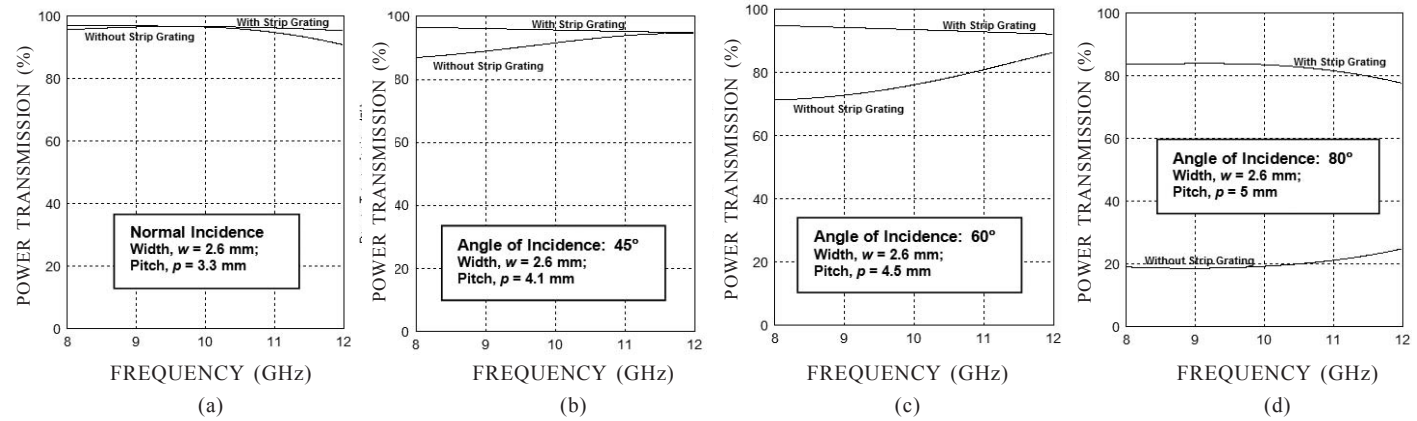

Figure 2. Power transmission characteristics of A-sandwich radome with metallic strip gratings embedded in the mid-plane of the core and A-sandwich alone (Configuration 1) at normal incidence, 45°, 60°, and 80°. (Polarization: Perpendicular).

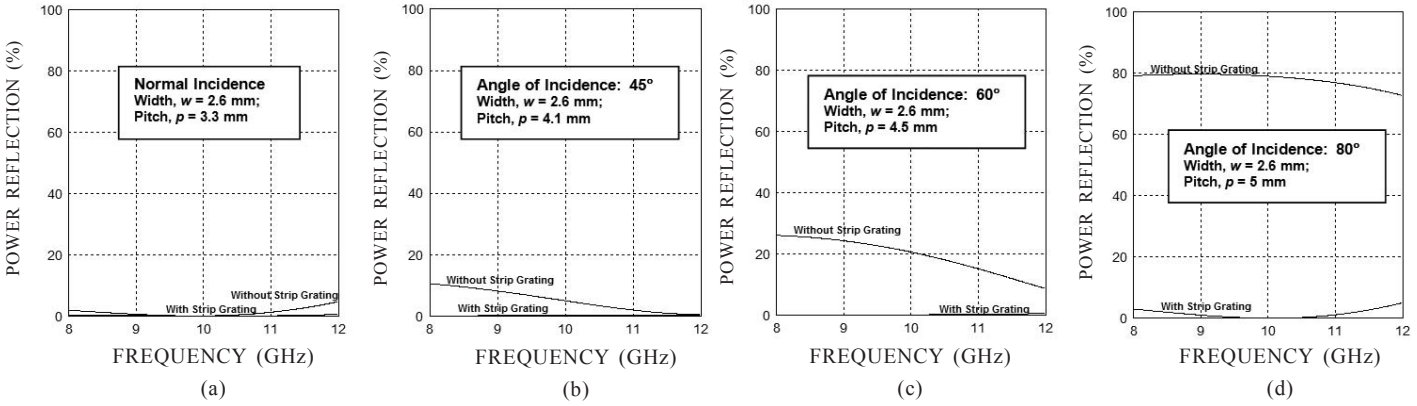

Figure 3. Power reflection characteristics of A-sandwich radome with metallic strip gratings embedded in the mid-plane of the core and A-sandwich alone (Configuration 1) at normal incidence, 45°, 60° and 80°. (Polarization: Perpendicular).

Table 1. Design parameters of metallic strip gratings

Type of configurations	Angle of incidence (Deg)	Polarization	Optimum width, *w* (mm)	Optimum pitch, *p* (mm)
Configuration 1	0	-	2.6	3.3
	45	Perpendicular	2.6	4.1
	60	Perpendicular	2.6	4.5
	80	Perpendicular	2.6	5.0
Configuration 2	0	-	2.7	2.8
	45	Perpendicular	2.7	2.8
	60	Perpendicular	2.7	2.8
	80	Perpendicular	2.7	2.8

A-sandwich alone at all incidence angles over the X-band. The power reflection characteristics of Configuration 2 are shown in Fig. 6. The A-sandwich wall embedded with metallic strip gratings shows very low power reflection as compared to that of the conventional structure. The power reflection for Configuration 2 is very low at normal incidence, 45°, and 60°. However, the power reflection of the conventional structure increases drastically at high incidence angle 80°. The insertion phase delay characteristics of Configuration 2 are shown in Fig. 7. It is observed that the IPD of the A-sandwich wall embedded with metallic strip gratings for Configuration 2 is higher than that of A-sandwich alone at all incidence angles. It is desirable for reducing phase distortions and hence boresight error. .

Among the two configurations considered, Configuration

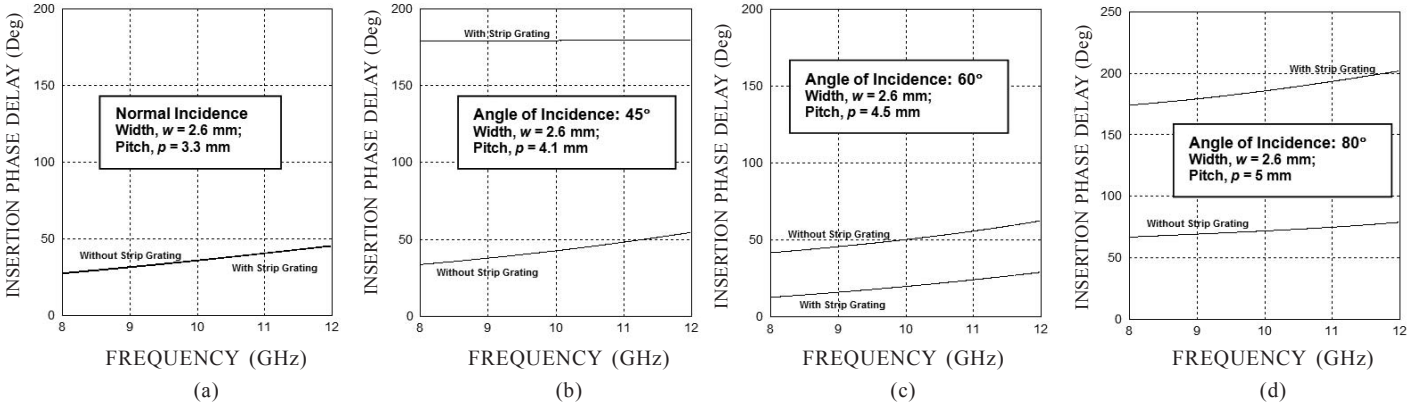

Figure 4. Insertion phase delay characteristics of A-sandwich radome with metallic strip gratings embedded in the mid-plane of the core and A-sandwich alone (Configuration 1) at normal incidence, 45°, 60°, and 80°. (Polarization: Perpendicular).

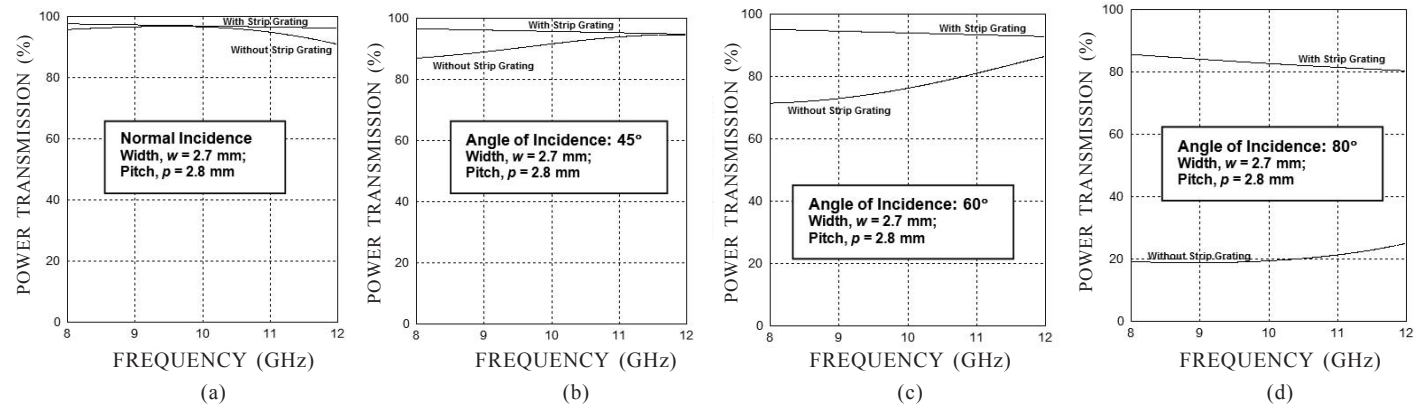

Figure 5. Power transmission characteristics of A-sandwich radome with metallic strip gratings embedded in each skin-core interface and A-sandwich alone (Configuration 2) at normal incidence, 45°, 60°, and 80°. (Polarization: Perpendicular).

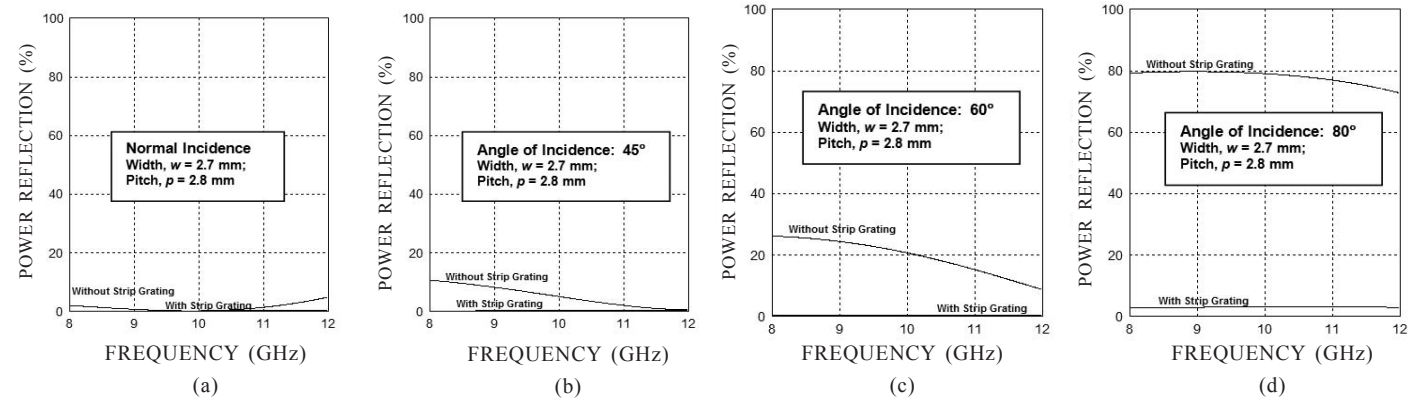

Figure 6. Power reflection characteristics of A-sandwich radome with metallic strip gratings embedded in each skin-core interface and A-sandwich alone (Configuration 2) at normal incidence, 45°, 60°, and 80°. (Polarization: Perpendicular).

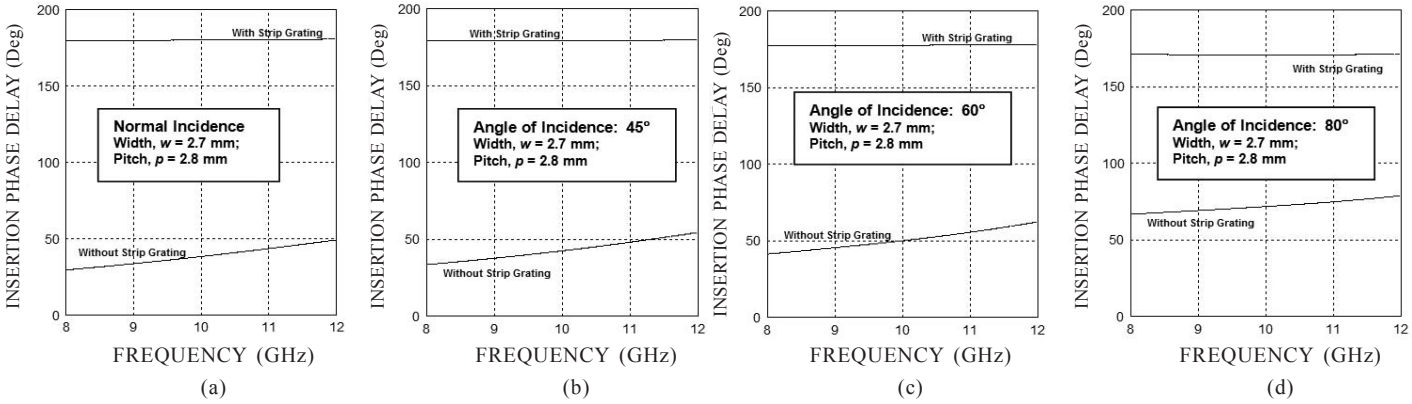

Figure 7. Insertion phase delay characteristics of A-sandwich radome with metallic strip gratings embedded in each skin-core interface and A-sandwich alone (Configuration 2) at normal incidence, 45°, 60°, and 80°. (Polarization: Perpendicular).

1 has better EM performance characteristics as compared to Configuration 2. The average power transmission efficiency (around 85 per cent) for Configuration 1, while that of Configuration 2 is around 82 per cent. Further, the average power reflection for Configuration 1 is nearly zero at high incidence angle 80°, while it is around 5 per cent for Configuration 2. At normal incidence, IPD of Configuration 2 is much higher than that of Configuration 1, indicating more phase distortions.

4. CONCLUSIONS

The application of metallic strip gratings for improving the EM performance characteristics of A-sandwich radome over X-Band is established in this work. It is observed that the novel A-sandwich wall configurations (Configuration 1 and Configuration 2) offer better EM performance characteristics as compared to the conventional A-sandwich wall with optimized core thickness. Considering the EM performance characteristics, Configuration 1 is preferable to Configuration 2. Further regarding fabrication aspects, Configuration 1 is desirable as only one set of strip grating has to be embedded in the structure. The present work also shows that A-sandwich wall with metallic strip gratings is a better choice for both the normal-incidence (i.e., cylindrical or spherical) radomes, and the highly streamlined (e.g. conical, ogival) nosecone radomes.

REFERENCES

1. Robinson, L.A. Electrical properties of metal loaded radomes. WADD Technical Report. Report No. 60-84, 1960.
2. Walton, Jr. J.D. Techniques for airborne radome design. AFAL Report. Report No. 45433, 1966, 105-108.
3. Crone, G.A.E.; Rudge, A.W. & Taylor, G.N. Design and performance of airborne radomes: A review. *IEE Proc.*, 1981, **128**(7), 451-464.
4. Cary, R.H.J. Radomes, *In* The Handbook of Antenna Design. Peter Peregrinus, London, 1982.
5. Frenkel, A. Thick metal dielectric window. *Electronics Letters*, 2001, **37**(23), 1374-1375.
6. Munk, B.A. Frequency selective surfaces - Theory and design. Wiley, New York, 2005.
7. Lin, B.-Q.; Li, F.; Zheng, Q.-R. & Zen, Y.-S. Design and simulation of a miniature thick-screen frequency selective surface radome. *Progress Electromagnetics Research*, 2009, **138**, 537-553.
8. Nair, R.U.; Madhumitha, J. & Jha, R.M. Broadband EM performance characteristics of single square loop FSS embedded monolithic radome. *Int. J. Antenn. Propag.*, 2013, 1-8.
9. Latrach, M.; Rmili, H.; Sabatier, C.; Seguenot, E. & Toutain, S. Design of a new type of metamaterial radome at low frequencies. *Microwave Optical Technol. Letters*, 2010, *52*(5), 1119-1123.
10. Basiry, R.; Abiri, H. & Yahaghi, A. Electromagnetic performance analysis of omega type metamaterial radome. *Int. J. RF Microw. Comput. Aided Eng.*, 2011, **21**(6), 665-673.
11. Narayan, S.; Shamala, J.B.; Nair, R.U. & Jha, R.M. Electromagnetic performance analysis of novel multiband metamaterial FSS for millimeter wave radome applications. *Computers, Materials Continua*, 2012, **31**(1), 1-16.
12. Kozakoff, D.J. Analysis of radome enclosed antennas. Artech House, Norwood, 2010.
13. Chen, F.; Shen, Q. & Zhang, L. Electromagnetic optimal design and preparation of broadband ceramic radome material with graded porous structure. *Progress Electromagnetics Research*, 2010, **105**, 445-461.
14. Pei, Y.M.; Zeng, A.M.; Zhou, L.C.; Zhang, R.B. & Xu, K.X. Electromagnetic optimal design for dual-band radome wall with alternating layers of staggered composite and Kagome lattice structure. *Progress Electromagnetics Research*, 2012, **122**, 437-452.
15. Lee, C.K. & Langley, R.J. Equivalent-circuit models for frequency-selective surfaces at oblique angles of incidence. *IEE Proc.*, Pt. H, 1985, **18**(6), 395-399.

CONTRIBUTORS

Dr Raveendranath U. Nair received his MSc and PhD in Physics (Microwave Electronics) from the School of Pure and applied Physics, Mahatma Gandhi University, Kerala, India, in 1989 and 1997, respectively. Since September 1999 he has been working as Scientist at the Centre for Electromagnetics in CSIR-NAL, Bangalore, India where currently he is a principal scientist. He has authored/co-authored over 100 research publications including journal papers, symposium papers and technical reports. His research interests include computational electromagnetics, EM design, analysis and performance measurements of radomes, metamaterials, frequency selective surfaces, EM material characterization techniques.

Ms J. Madhumitha obtained the BE (Electronics and Communication) from Anna University, Chennai, in 2005. She is currently working as a Technical Manager in Sterling Electronics at Tiruchirappalli, Tamilnadu, India. She was earlier working as a Project Engineer at the Centre for Electromagnetics, CSIR-National Aerospace Laboratories (CSIR-NAL), Bangalore, India. Her research interests area are Radomes and EM material characterization.

Dr Rakesh Mohan Jha obtained a dual degree in BE (Hons.) EEE and MSc Physics from BITS Pilani (Raj.), in 1982 and PhD from Department of Aerospace Engineering, Indian Institute of Science, Bangalore, in 1989. He is currently a Chief Scientist and Head of Centre for Electromagnetics at CSIR-National Aerospace Laboratories, Bangalore. He is also concurrently Professor and Associate Dean of the Academy of Scientific and Innovative Research, New Delhi. His active areas of research are in the domain of computational electromagnetics for aerospace applications; these include GTD/UTD, 3-D ray tracing and surface modelling, aerospace antennas and radomes, radar cross section (RCS) studies including active RCS reduction, radar absorbing materials and radar absorbing structures, and metamaterials for aerospace applications. He has published more than 400 scientific research papers and technical reports.